Dielectric Normal Mode Process in Undiluted *cis*-Polyisoprene

Keiichiro Adachi* and Tadao Kotaka

Department of Macromolecular Science, Faculty of Science, Osaka University, Toyonaka, Osaka 560, Japan. *Received May 3, 1984*

ABSTRACT: Dielectric measurements were carried out on ten undiluted *cis*-polyisoprene (*cis*-PI) samples with different molecular weights. *cis*-PI exhibited dielectric relaxation due to the fluctuation of the end-to-end distance, termed the "normal mode process", as well as dielectric relaxation due to the segmental mode process. From the magnitudes of the dispersion, the parallel and perpendicular components of the dipole moment along the chain contour were calculated to be 0.17 ± 0.03 and 0.21 D, respectively. The relaxation time for the normal mode process, τ_{Dn}, was quite sensitive to the molecular weight M and exhibited an M dependence similar to that for the mechanical relaxation time of *cis*-PI. Below a characteristic molecular weight M_c (=10^4), τ_{Dn} was proportional to M^2, in agreement with the Rouse theory, but above M_c, τ_{Dn} was proportional to $M^{3.7}$. The latter result was explained by the tube disengagement process proposed by de Gennes. The distribution of τ_{Dn} became broader with molecular weight, tailing toward the high-frequency side. This behavior was also explained in terms of the tube theory.

Linear flexible polymers in which the dipole moments are aligned in the direction parallel to the chain contour exhibit a dielectric relaxation due to fluctuation of the end-to-end distance.[1,2] Such a relaxation process was referred to as the "dielectric normal mode process",[3] because such motions in dilute solutions were described by the normal modes in the Rouse–Zimm theory.[4,5] Recently, we found that undiluted *cis*-polyisoprene (*cis*-PI) exhibits the dielectric normal mode process and have made a preliminary report in our previous communication.[6] In this paper, we report the dielectric properties of undiluted *cis*-PI in detail.

Principally, two different types of information about the properties of chain molecules can be obtained[7] from the dielectric data on the normal mode process, i.e., the dynamic properties related to the end-to-end fluctuation and the static properties such as the dipole moment and mean square length $\langle r^2 \rangle$ of the end-to-end vector. Dynamic aspects have been studied by several authors for undiluted polymers with low molecular weight[8,9] and dilute solutions.[3,10-12] Since polymer chains are not entangled in these systems, their dielectric behavior has been explained by the Rouse–Zimm theory.[4,5] Stockmayer[1] suggested as early as 1967 that the normal mode process in entangled systems was an intriguing future problem. However, this problem has not yet been clarified. In our previous communication,[6] the relaxation time for the normal mode process in bulk *cis*-PI with molecular weight M above a characteristic molecular weight M_c (of approximately 10^4) was found to be proportional to the 3.7 ± 0.2 power of the molecular weight. Since this behavior is similar to the well-known 3.4 power law for the maximum viscoelastic relaxation time in entangled systems,[13,14] the experimental result suggests that the effect of entanglement on the dielectric normal mode process may also be described by the tube theory proposed by de Gennes[15,16] and developed by Doi and Edwards.[17] In this paper, we attempt to explain the dielectric relaxation time and the relaxation spectra in terms of the tube theory.

The magnitude of the dielectric dispersion for the normal mode process is theoretically predicted to be proportional to $\langle r^2 \rangle$.[5,7] However, few experimental studies have been made to establish this relation. For such an analysis of the static properties, we need to determine the parallel dipole moment. In this study, we have calculated the parallel dipole moment based on the value of $\langle r^2 \rangle$ determined from the intrinsic viscosity.

In addition to the data on the normal mode process, we obtained information on the segmental mode process due to local motions.[18] Although many authors have made dielectric studies on the segmental motion, comparison between the segmental mode and normal mode processes have rarely been made. We compared the relaxation times for the both processes.

Table I
Characteristics of the *cis*-PI Samples

code	$10^{-4}M_w$	M_w/M_n	microstructure, mol %		
			cis-1,4	trans-1,4	vinyl-3,4
PI-01	(0.10)[a]		77.8	18.2	4.0
PI-05	0.48	1.5	80.0	16.3	3.7
PI-09	0.86	1.29	81.2	15.5	3.3
PI-11[b]	1.10	1.17	83.4	13.0	3.7
PI-16[b]	1.62	1.23	74.3	21.3	4.4
PI-20[b]	2.04	1.20	71.9	22.4	5.6
PI-42[b]	4.19	1.34	83.9	12.3	3.8
PI-59[b]	5.89	1.33	79.4	18.0	2.6
PI-102	10.2	1.18	78.3	18.7	3.0
PI-128[b]	12.8	1.37	81.1	14.3	4.7

[a] M_n value. [b] Samples used in the previous study.[6] For some of these samples, the code was changed according to the M_w values.

Experimental Section

Materials. Preparation and characterization of *cis*-PI samples were described previously.[6] In addition to the seven samples used in the previous study,[6] we prepared three samples with molecular weight lower than 1×10^4 and one sample (PI-102) having a relatively narrow molecular weight distribution. All samples were prepared by anionic polymerization in *n*-pentane at ca. 25 °C and, especially for the last one, by employing the procedure called "seeding".[19] Table I shows the characteristics of the samples used in this study. It is necessary to check the content of polar impurities in the samples since impurities such as carbonyl groups would strongly affect the dielectric constant. We attempted to measure the content of C=O groups by infrared spectroscopy. However, the absorption band due to C=O was not observed around 1720 cm^{-1}. As described later, the dipole moment of the monomeric unit calculated from the dielectric data is in agreement with that of propene, indicating that the present samples do not contain polar impurities.

Methods. Complex dielectric constants were measured by using a capacitance cell designed for viscous liquid samples.[20] After the sample was introduced into the cell, the container was evacuated and then filled with helium in order to avoid oxidation and contamination with water. Bridges for dielectric measurements were described previously.[3,6]

Results

Frequency Dependence of the Dielectric Constant and Loss. The frequency dependences of the dielectric constant ϵ' and the loss factor ϵ'' for the samples with molecular weights 1.1×10^4 to 1.2×10^5 were shown previously.[6] Figure 1 shows ϵ' and ϵ'' measured at 320 K for

0024-9297/85/2218-0466$01.50/0

Table II
Vogel-Tamman Parameters A, B, and T_0, Defined by Eq 1 for the Segmental and Normal Mode Processes

code	segmental mode			normal mode		
	A	B	T_0	A	B	T_0
PI-01	11.44	489.3	161.3	9.30	551.6	157.0
PI-05	11.15	422.5	173.8	8.50	530.2	168.4
PI-11	11.03	413.0	174.6	7.71	510.2	169.5
PI-42	11.24	438.3	175.9	5.34	495.0	175.9
PI-102	11.40	445.0	175.0	3.75	495.0	175.9

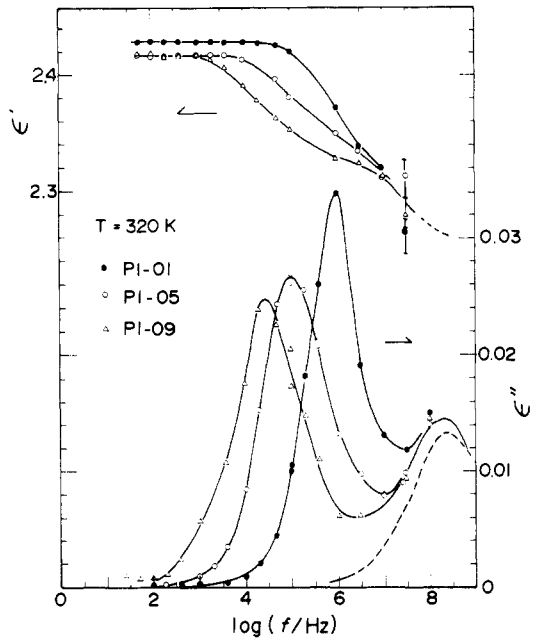

Figure 1. Frequency dependence of ϵ' and ϵ'' at 320 K for PI-01, PI-05, and PI-09. The dashed line represents the curve estimated by eq 2 for the segmental mode process of PI-01.

three samples with molecular weight below 10^4. The loss maxima around 100 kHz are due to the normal mode process, while the increase in ϵ'' around 100 MHz can be attributed to the segmental motion. It should be noted that these loss curves for the normal mode process are sharper than those for the high molecular weight *cis*-PI samples.

Relaxation Times. It was shown previously that the frequency of the loss maximum for the normal mode process, f_{mn}, and that for the segmental motion, f_{ms}, vary with temperature in almost the same manner.[6] Since log f_m was not linear against $1/T$, we expressed f_m by using the Vogel–Tamman equation[21,22]

$$\log f_m = A - B/(T - T_0) \quad (1)$$

Here, A, B, and T_0 are parameters. The values of these parameters for the representative samples are listed in Table II. The parameters for f_{mn} were somewhat ambiguous because of the experimentally limited range of frequency. Especially for samples with $M > 4 \times 10^4$, several sets of the values of A, B, and T_0 could equally well reproduce the f_{mn} vs. T^{-1} plots. Thus we arbitrarily chose T_0 to be the same as that for the segmental mode of PI-42.

The dielectric relaxation times for the normal mode process, τ_{Dn}, were calculated by using the relation $\tau_{Dn} = 1/(2\pi f_{mn})$ at 320, 300, 273.2, and 250 K by interpolation or extrapolation of the Arrhenius plots. The results are listed in Table III. The molecular weight dependence of τ_{Dn} at 320 K is shown in Figure 2.

In contrast to τ_{Dn}, the relaxation time for the segmental modes τ_{Ds} was almost independent of M_w for samples with $M_w > 10^4$ and decreased slightly with decreasing M_w for samples with $M_w < 10^4$ as shown in the Arrhenius plot

Table III
Values of log τ_{Dn} at Various Temperatures[a]

code	320 K	300 K	273.2 K	250 K
PI-01	−6.75	−6.28	−5.35	−3.98
PI-05	−5.80	−5.27	−4.22	−2.80
PI-09	−5.26	−4.68	−3.60	−2.32
PI-11	−5.10	−4.65	−3.58	−2.25
PI-16	−4.70	−4.13	−3.10	−1.17
PI-20	−4.32	−3.73	−2.60	(−1.00)
PI-42	−2.70	−2.15	−1.20	(0.54)
PI-59	−2.35	(−1.76)	(−0.65)	(0.94)
PI-102	−1.17	(−0.62)	(0.48)	(2.07)
PI-128	−1.01	(−0.46)	(0.64)	(2.23)

[a] The values in parentheses are those extrapolated by the Vogel–Tamman equation.

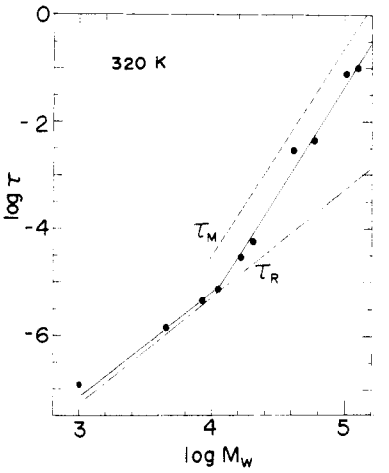

Figure 2. Molecular weight (M_w) dependence of the relaxation time for the normal mode process τ_{Dn}. For the plot at log M = 3 (PI-01), we used M_n. The dashed line represents the maximum mechanical relaxation time reported in ref 23 and 24. The dot–dash line represents the maximum relaxation time in the Rouse theory.

reported previously.[6] This trend can be ascribed to the increasing content of free volume created by the chain ends. The difference in f_{ms} between the low and high molecular weight samples increased with decreasing M_w and also with decreasing temperature.

The Arrhenius plots for f_{mn} and f_{ms} varied in an almost parallel fashion.[6] To test this quantitatively, we calculated the ratio τ_{Dn}/τ_{Ds} at various temperatures by using the Vogel–Tamman relations. For example, the ratio τ_{Dn}/τ_{Ds} for PI-05 at 220 K is 3.3 times greater than that at 320 K. Similar variations of the ratio were also observed for PI-01 and PI-11.

Master Curve. The similar dependence of τ_{Dn} and τ_{Ds} on temperature implies that the ϵ' and ϵ'' curves at various temperatures are superposable.[13] We constructed master curves for representative samples as follows. The ϵ'' curves were shifted from T to a reference temperature T_r after being multiplied by a factor of $T\rho(T_r)/T_r\rho(T)$, since the relaxation strength is approximately proportional to $\rho(T)/T$. We used density data reported by Nemoto et al.[23] On the other hand, the ϵ' curves were shifted in two steps

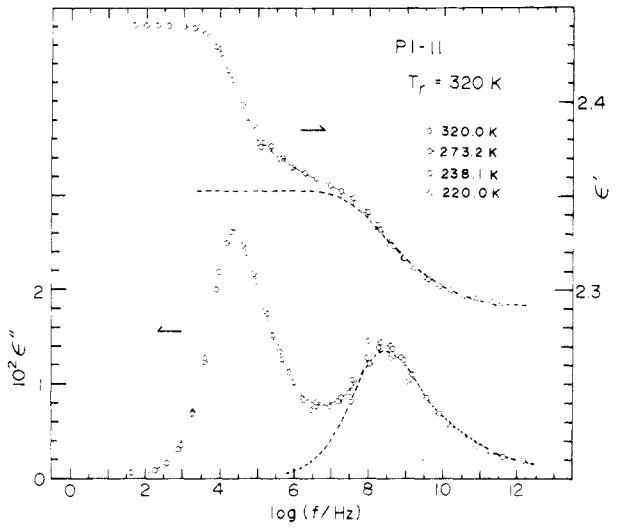

Figure 3. Master curve of ϵ' and ϵ'' for PI-11 at 320 K.

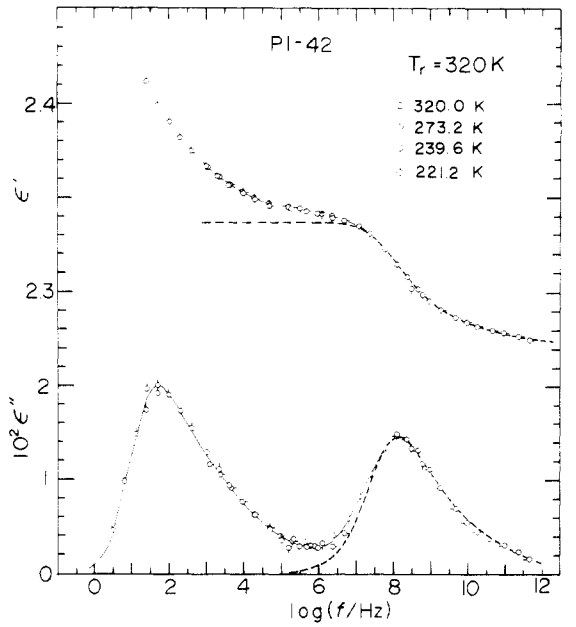

Figure 4. Master curve of ϵ' and ϵ'' for PI-42 at 320 K.

because the relaxing component is proportional to $\rho(T)/T$, but the nonrelaxing component due to electronic polarization is proportional only to $\rho(T)$. Thus, first the ϵ' curve was multiplied by $T\rho(T_r)/T_r\rho(T)$ and was shifted along the abscissa using the same shift factor as for the ϵ'' curve. Second it was shifted along the ordinate so that the best superposition was achieved. The master curves thus constructed for PI-11, PI-42, and PI-102 are shown in Figures 3, 4, and 5, respectively. We note that the width of the loss curve for the normal mode process increases with molecular weight.

Magnitude of Dielectric Dispersion. The magnitude of the dielectric dispersion $\Delta\epsilon = \epsilon_0 - \epsilon_\infty$ for the segmental mode process was determined from the Cole–Cole plot, where ϵ_0 and ϵ_∞ denote relaxed and unrelaxed dielectric constants, respectively. Since the Cole–Cole diagrams were of skewed arc shape, we fitted the data at 320 K to the Havriliak–Negami equation[25]

$$\epsilon^*(\omega) - \epsilon_\infty = \Delta\epsilon/[1 + i(\omega\tau_0)^{1-\alpha}]^\beta \qquad (2)$$

where ϵ^* is the complex dielectric constant, ω is the angular frequency, τ_0 is the nominal relaxation time, and α and β are parameters. According to the procedure described by Havriliak and Negami,[25] the parameters α, β, and τ_0 were

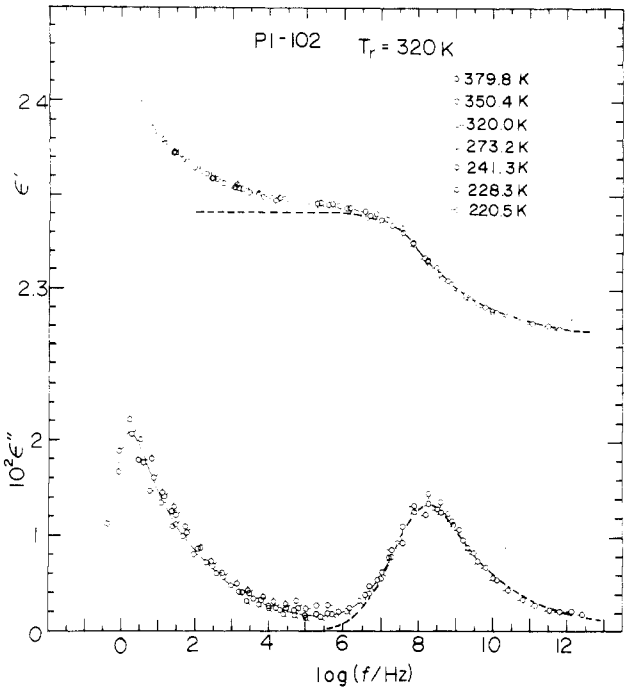

Figure 5. Master curve of ϵ' and ϵ'' for PI-102 at 320 K.

Table IV
Parameters in the Havriliak–Negami Equation for the Segmental Mode Process

code	ϵ_0	ϵ_∞	α	β	$10^9\tau_0$, s
PI-42	2.337	2.272	0.182	0.357	3.48
PI-102	2.341	2.276	0.213	0.327	3.40

Table V
Magnitude of Dielectric Dispersion $\Delta\epsilon_n$ for the Normal Mode Process

code	$10^2\Delta\epsilon_n$	code	$10^2\Delta\epsilon_n$
PI-01	7.8	PI-11	8.57
PI-05	8.1	PI-40	8.23
PI-09	7.8	PI-102	8.30

determined for PI-42 and PI-102 as listed in Table IV.

Since the accuracy of ϵ' measured in the low-frequency region was relatively poor, $\Delta\epsilon$ for the normal mode process, $\Delta\epsilon_n$, was determined from the area under the loss curve. As shown in Figures 1, 3, and 4, the loss curves due to the segmental mode and normal mode processes partially overlap. We separated them as follows. Since the segmental mode is not sensitive to molecular weight, we assumed that the Havriliak–Negami parameters, α and β in eq 2, for low molecular weight samples are the same as those for PI-102. For their τ_0, we corrected that for PI-102 in such a way that τ_0(PI-05)/τ_0(PI-102) = f_{ms}(PI-102)/f_{ms}(PI-05). In this way, the ϵ' and ϵ'' curves for the segmental mode process in the overlapping region were estimated as shown by dashed lines in Figures 1, 3, and 4. The results of calculation of $\Delta\epsilon_n$ are listed in Table V.

Direct determination of ϵ_0 and ϵ_∞ in the ϵ' vs. log f curve was possible only for PI-11. As shown in Figure 3, the value of ϵ_∞ for the normal mode process was assumed to be equal to ϵ_0 for the segmental mode process. Thus, $\Delta\epsilon_n$ by this method amounted to 0.088, in agreement with the value determined from the ϵ'' curve.

Discussion

Dipole Moment. The dipole moment of the monomeric unit can be decomposed into components parallel to, μ_1, and perpendicular to, μ_2, the chain contour. They are responsible for the normal mode and the segmental mode

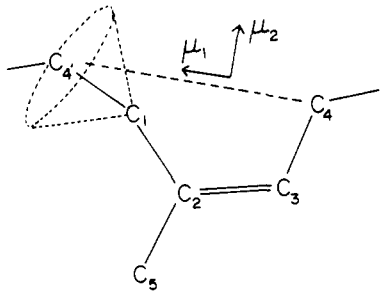

Figure 6. Molecular structure of the monomer unit of *cis*-polyisoprene.

processes, respectively. One of the methods to determine the dipole moment is to calculate the vectorial sum of the individual bond moments. Unfortunately, no reliable data for the moment of C–CH_3 and the –C=C(CH_3)– double bond have been reported. Therefore, we attempted to determine these components directly from the experimental data.

For a polymer with the parallel dipole moment μ per unit contour length, $\Delta\epsilon_n$ is given by[5,7]

$$\Delta\epsilon_n = 4\pi n_p \mu^2 \langle r^2 \rangle F/(3k_B T) \tag{3}$$

where n_p is the number of polymer molecules in a unit volume, F is the ratio of internal and external electric fields, and $k_B T$ has the usual meaning. It is noted that $\Delta\epsilon_n$ is proportional to $\langle r^2 \rangle/M$, since n_p is proportional to $1/M$. To calculate μ, it is necessary to estimate the values of $\langle r^2 \rangle$ and F. Since the conformation of polymer molecules in the undiluted state is equivalent to that in the unperturbed state, we estimated the value of $\langle r^2 \rangle/M$ to be 0.70 Å^2 from the intrinsic viscosity data $[\eta]$ in a Θ solvent[27] by using the Flory–Fox equation[26]

$$[\eta] = \Phi[\langle r^2 \rangle/M]^{3/2} M^{1/2} \tag{4}$$

with 2.5×10^{21} (in dL/g units) for the universal constant Φ.

For F in dilute solutions, Stockmayer and Baur[7] used the Lorentz field[28] given by

$$F = (\epsilon_s + 2)^2/9 \tag{5}$$

where ϵ_s is the static dielectric constant of the solvent. For undiluted polymers, ϵ_s should be replaced by the unrelaxed dielectric constant ϵ_∞ (=2.35) for the normal mode process. Although the factor F given by eq 5 is correct for simple molecules, its application to the normal mode process has not been fully justified. The result of our recent study on the concentration dependence of ϵ' for dilute solutions of poly(2,6-dichlorophenylene oxide) in *o*-dichlorobenzene and in chlorobenzene indicated that F in the case of the normal mode process has a value close to unity.[29] Although the exact functional form of F is unknown at present, we consider that F given by eq 5 may be an overestimate, while $F = 1$ may be an underestimate. From the average values of $\Delta\epsilon_n$ given in Table V and the density (=0.890 g/cm^3 at 320 K),[23] we calculated μ (in cgs esu) to be 3.31×10^{-12} by eq 5 and 4.80×10^{-12} by assuming $F = 1$.

In order to estimate μ_1 from the value of μ, we need to define the length, b, of the monomeric unit. Figure 6 shows the structure of the monomeric unit, and the average length from C_4 to $C_{4'}$ may be taken as b. Mark[30] indicated that the potential energy with respect to the angle ϕ of internal rotation around the C_3–C_4 bond is minimum at $\phi = 0$ and $\phi = \pm 60°$, where $\phi = 0$ corresponds to the state that the C_2=C_3 and C_4–C_1 bonds are in the trans conformation. Mark indicated that the statistical weight for the conformation at $\phi = \pm 60°$ is greater than that at 0° by a factor of 10. By using the values of statistical weight, and the bond lengths and angles employed by Mark,[30] we estimated the average length from C_4 to $C_{4'}$ to be 0.42 nm. In this way, μ_1 (=μb) was calculated to be 0.14 D with the Lorentz field (eq 5) and 0.20 D with $F = 1$.

The perpendicular component μ_2 per repeat unit was calculated by using the Onsager equation[18] under the assumption that there is no short-range interaction between the neighboring perpendicular dipoles

$$\Delta\epsilon_s = \frac{4\pi n_p x \mu_2^2}{9k_B T} \frac{\epsilon_0(\epsilon_\infty + 2)^2}{2\epsilon_0 + \epsilon_\infty} \tag{6}$$

where x is the degree of polymerization. From the value of $\Delta\epsilon_s$ for PI-102, we obtained $\mu_2 = 0.21$ D. The net dipole moment of the repeat unit, which is the vectorial sum of μ_1 and μ_2, amounts to 0.25 D under the Lorentz field approximation and to 0.29 D under the $F = 1$ vacuum approximation. These values are comparable to the dipole moment of propene (0.35 D).[31] It is noted that since we have determined the dipole moments based on the data of $\Delta\epsilon_n$, the dipole moment thus calculated is an average of the dipole moment for cis, trans, and vinyl units incorporated in the *cis*-PI samples.

As to the origin of the parallel dipole moment, we consider that the C=C double bond in an isoprene unit has a relatively strong bond moment due to the presence of the methyl group. A calculation of the electron density by means of the molecular orbital method confirmed this assumption.[32] Thus, we may expect that a trans-1,4 unit also has a parallel dipole moment of similar magnitude to that of the cis unit. The details of the calculation will be reported elsewhere.

Molecular Weight Dependence of the Relaxation Time. As shown in Figure 2, the slope of the log τ_{Dn} vs. log M_w plot in the range of molecular weight above 10^4 is 3.7 ± 0.2. This behavior is similar to the molecular weight dependence of the maximum mechanical relaxation time, τ_M, in the entangled system, known as the 3.4 power law.[13,14] The dashed line in Figure 2 shows the maximum mechanical relaxation time reported by Nemoto et al.[23,24] for *cis*-PI samples having a cis content similar to that of the present samples. From the fact that τ_{Dn} and τ_M roughly coincide, we may conclude that the dielectric normal mode process originates from a mechanism similar to mechanical relaxations. The slope of the log τ_{Dn} vs. log M_w curve changes at $M = 10^4$, which agrees with the characteristic molecular weight M_c for the log (melt viscosity) vs. log M curve for *cis*-PI.[23,24] Thus, M_c for τ_{Dn} also coincides with that for τ_M.

In the range $M < M_c$, τ_{Dn} is proportional to $M^{2.0}$, in accordance with Rouse theory. Thus, there is no effect of entanglement and the Rouse modes prevail in this range. The maximum dielectric relaxation time τ_R for the Rouse modes is given by [1,5]

$$\tau_R = 12M\eta/(\pi^2 \rho RT) \tag{7}$$

As shown in Figure 2, τ_{Dn} below M_c agrees with τ_R. Baur and Stockmayer[8] reported that undiluted poly(propylene oxide) with low molecular weight also exhibits the Rouse modes. From these results, we conclude that regardless of the entanglement effect, the dielectric relaxation time for the normal mode process is approximately the same as the mechanical maximum relaxation time.

Application of Tube Model. Owing to the similarity in the behavior of the dielectric and mechanical relaxation times, we considered that the dielectric relaxation in *cis*-PI with $M > M_c$ should be explained by the tube theory which

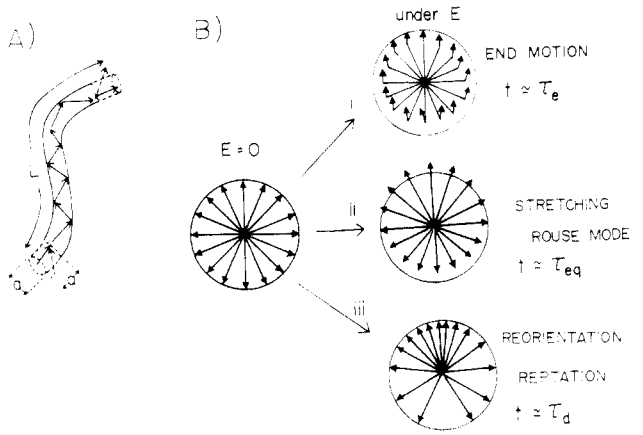

Figure 7. (A) Tube model. (B) Schematic diagram representing the three mechanisms of polarization. In the absence of an electric field, the orientation of the end-to-end vectors is isotropic as represented in this figure. By application of a field, the chain ends orient most rapidly with a relaxation time τ_e as shown by diagram i. Stretching of the chain causes polarization as shown by diagram ii with the relaxation time τ_{eq}. Finally, the reorientation of the chain occurs with relaxation time τ_d as shown by diagram iii. It should be noted that since the chain is confined in the tube, reorientation is achieved only by tube disengagement.

was proposed by de Gennes[15] and demonstrated by Doi and Edwards[1m] to successfully explain the mechanical relaxations in entangled systems.

We introduce a model that a chain having a dipole moment proportional to its end-to-end distance is confined in a tube as shown in Figure 7A. The chain diffuses along the tube by a motion called reptation. After the chain moves out of the tube it enters another new tube, and as a result, the end-to-end vector changes its direction. The dielectric relaxation due to such a motion may be described in terms of the autocorrelation function of the polarization vector **P**, written as

$$\langle \mathbf{P}(0)\mathbf{P}(t)\rangle = \mu^2\langle \mathbf{r}(0)\mathbf{r}(t)\rangle \tag{8}$$

where the brackets indicate the ensemble average, t is the time, and μ has the same meaning as in eq 3. As is well-known, the frequency dependence of the complex dielectric constant $\epsilon^*/4\pi$ is given by the Fourier transform of the time derivative of the correlation function.[35] According to de Gennes,[15] the correlation function of $\mathbf{r}(t)$ due to the reptation mechanism is expressed as

$$\langle \mathbf{r}(0)\mathbf{r}(t)\rangle = \langle r^2\rangle \sum_{\substack{p \\ \text{odd}}} (1/p^2)\exp(-t/\tau_p) \tag{9}$$

$$\tau_p = \tau_d/p^2 \tag{10}$$

where τ_d is the maximum relaxation time for the tube disengagement process. Since the contribution of the higher order terms with $p > 3$ is much smaller than that of the fundamental mode, $p = 1$, we regarded that the dielectric relaxation time is approximately given by τ_d, i.e., the mode with $p = 1$. The theory[15,16] predicts that τ_d is proportional to the 3.0 power of molecular weight. Thus, the tube theory explains semiquantitatively the molecular weight dependence of τ_{Dn} for the samples with $M > M_c$. The slight but significant difference between the actual power and 3.0 of the model was originally pointed out for the mechanical relaxations and explained by Doi by considering the fluctuation of the arc length of the primitive chain confined in the tube.[34]

Dielectric Relaxation Spectra for Normal Mode Process. As discussed in the previous section, the relaxation time for the normal mode process of *cis*-PI may be explained semiquantitatively by the tube disengagement model. However, one might consider that the end-to-end stretching mode (Rouse mode) also contributes partly to the polarization even in the entangled systems. As shown in Figures 1, 3, 4, and 5, the width of the loss curve for the normal mode process, which reflects the distribution of the relaxation time, becomes broad and tails to the high-frequency side with increasing molecular weight. Obviously this increment in the distribution of relaxation time cannot be attributed to the change in the distribution of molecular weight because the M_w/M_n ratios for PI-11 and for PI-102 are nearly the same. These results indicate the presence of processes having shorter relaxation times than tube disengagement process.

To explain these broad relaxation spectra for the normal mode process, we consider motions of a chain molecule confined in a tube with a diameter a and an arc length L, following Doi and Edwards[17] (Figure 7A). Here, a^2 is equal to the mean square end-to-end distance of a submolecule with the molecular weight between entanglements M_e (= $M_c/2$) and L is equal to aM/M_e.

When a unit internal electric field is applied to the chain at time $t = 0$, the following three types of dielectric responses may occur: (1) reorientation of the subchains with molecular weight M_e at both ends of the chain; (2) stretching or contraction of the chain within the tube; and (3) reorientation of the end-to-end vector by the tube disengagement or reptation process. These responses are schematically shown in Figure 7B.

The submolecules of size M_e at the chain ends are free from the constraint by entanglement. Therefore, the reorientation of the ends may occur most rapidly as illustrated in Figure 7. We assume that the junctions of the end subchains found at a distance corresponding to the chain length M_e from the ends are fixed by a slip link[17] within the time scale of the end motion. The chain ends reorient by rotational motion around the slip links and cause a change in the polarization. The relaxation time for this process, τ_e, should be the same as that for the overall rotation of a random coil with size $2M_e$ (see Figure 7). Since the relaxation time for the overall rotation of a random coil is close to the relaxation time given by the Rouse theory,[1] τ_e may be approximately equal to $\tau_R(2M_e)$ and, therefore, may be given by

$$\tau_e = 4\tau_R(M_e) \tag{11}$$

According to the tube model, the maximum relaxation times for the second and the third processes τ_{eq} and τ_d are given by[17]

$$\tau_{eq} = N^2\tau_R(M_e) \tag{12}$$

$$\tau_d = N^3\tau_R(M_e) \tag{13}$$

where N is equal to M/M_e. For the sake of simplicity, we neglect the higher order modes (the modes with $p \geq 3$ in eq 9 and in the Rouse theory). If the stretching of the chain in the tube is taken into consideration, the effective tube length L decreases on account of the fluctuation of the chain length.[34] However, we assume that τ_d is given by the relaxation time without fluctuation of the chain length, since the exact functional form of τ_d for the chain with $M < 10M_c$ is complex.[34]

When the magnitudes of equilibrium polarization for the first, second, and third processes are p_1, p_2, and p_3, respectively, the time dependence of the autocorrelation function $\langle \mathbf{P}(0)\mathbf{P}(t)\rangle$ is given by

$$\langle \mathbf{P}(0)\mathbf{P}(t)\rangle = p_1\exp(-t/\tau_e) + p_2\exp(-t/\tau_{eq}) + p_3\exp(-t/\tau_d) \tag{14}$$

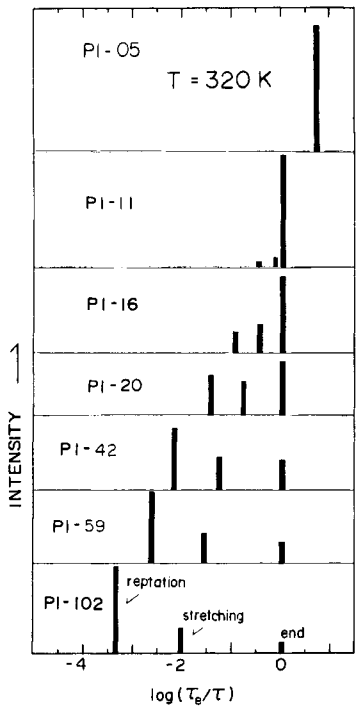

Figure 8. Dielectric relaxation spectra for the normal mode process at 320 K calculated by using the value of $\tau_R(M_e)$ and eq 12, 13, 16, 18, and 19.

Before evaluating p_1, p_2, and p_3, we note that the mean total polarization p ($=p_1 + p_2 + p_3$) is given by

$$p = \mu^2\langle r^2\rangle/(3k_BT) \tag{15}$$

It should be noted that this equation holds, regardless of the type of the distribution function of the chain ends. On the basis of eq 15, we may write p_1 as

$$p_1 = 2\mu^2a^2/(3k_BT) = 2p_0 \tag{16}$$

by replacing $\langle r^2\rangle$ by a^2 and considering the factor 2 due to the contribution from both ends. Here, p_0 is the magnitude of polarization for a Rouse chain with molecular weight M_e.

Since the polarization is proportional to the fluctuation of the dipole moment, p_2 should be proportional to the amplutide of the fluctuation in r^2 due to the stretching motion of the chain in the tube. Doi[36] suggested that p_2/p_3 is given by

$$p_2/p_3 = (1/N^{1/2})/(1 - 1/N^{1/2}) \tag{17}$$

because the fluctuation of the primitive chain length L is equal to $L/N^{1/2}$.[34] From eq 15–17, we obtain

$$p_2 = p_0(N - 2)/N^{1/2} \tag{18}$$

$$p_3 = p_0(N - 2)(1 - 1/N^{1/2}) \tag{19}$$

By Fourier transform of $d\langle \mathbf{P}(t)\mathbf{P}(0)\rangle/dt$, we obtain the complex dielectric constant ϵ^* as a sum of the Debye functions

$$\epsilon^*/4\pi n_p = p_1/(1 + i\omega\tau_e) + p_2/(1 + i\omega\tau_{eq}) + p_3/(1 + i\omega\tau_d) \tag{20}$$

where i^2 is -1 and n_p deonotes the number of the molecules.

On the basis of these equations, we calculated dielectric relaxation spectra at 320 K for the normal mode process. The results are shown in Figure 8. As shown in this figure, the theoretically derived relaxation spectra become broad with molecular weight, tailing toward the high-frequency side. This is in qualitative agreement with the experiment. Figure 9 shows the comparison of the ϵ'' curves at 320 K

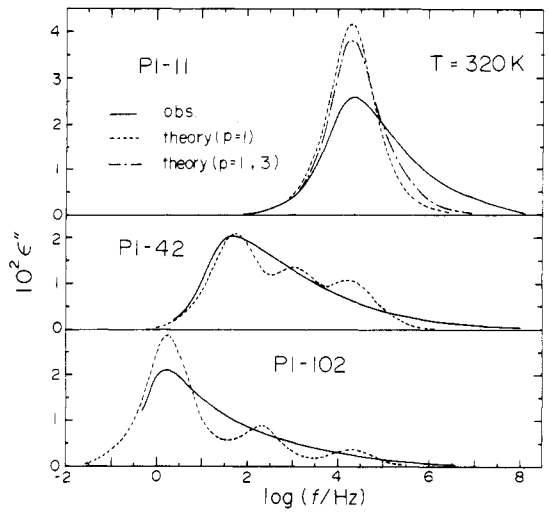

Figure 9. Comparison of the ϵ'' curves calculated by eq 20 (dashed line) and those observed for PI-11, PI-42, and PI-102 at 320 K. Dot–dash line represents the theoretical curve depicted by taking into account the third mode (p = 3) in the Rouse theory.[4]

calculated by using eq 20 and those for the normal mode process depicted from the master curves. Here we assumed that τ_d is equal to $1/(2\pi f_{mn})$ without using eq 13, since the actual τ_d is proportional $M^{3.7}$ instead of M^3. We also assumed that $4\pi n_p N p_0$ is equal to $\Delta\epsilon_n$. As shown in Figure 9, the theoretical ϵ'' curves show a fine structure but the experimental curves do not. Clearly, this discrepancy may be attributed to the oversimplification of the model used here. However, both curves are approximately in agreement. Thus, we can conclude that the tube model is satisfactory to describe, at least semiquantitatively, the molecular weight dependence of the distribution of relaxation times for the normal mode process.

Relationship between τ_{Dn} and τ_{Ds}. It has been shown that τ_{Dn}/τ_{Ds} is almost independent of temperature as observed for undiluted poly(propylene oxide).[8,9] This fact suggests that the frictional constant for the normal mode process is always proportional to that for the segmental mode process. Since τ_{Dn} changes with molecular weight, we examined the relationship between τ_{Ds} and $\tau_R(M_e)$, which is a reference relaxation time of τ_{Dn} as shown by eq 12 and 13.

It was reported that M_e for *cis*-PI is about 5000.[14,23,24] The present data indicate that $\tau_R(M_e) = 1.4 \times 10^{-6}$ s and $\tau_{Ds} = 1.0 \times 10^{-9}$ s. Thus the value of log $[\tau_R(M_e)/\tau_{Ds}]$ amounts to 3.15. It is interesting to compare this ratio with that for poly(propylene oxide). From the data reported by Baur and Stockmayer[8] and the value of M_c (=5800) for poly(propylene oxide),[37] we calculated log $[\tau_R(M_e)/\tau_{Ds}]$ to be 3.12 at 243 K, in good agreement with the ratio for *cis*-PI. Although there is a possibility that the agreement is accidental, these results suggest that the ratio of $\tau_R(M_e)$ and τ_{Ds} is a universal constant irrespective of the chemical structure of the monomer unit.

Conclusions

(1) The molecular weight dependence of the dielectric relaxation time for the normal mode process τ_{Dn} changed at a characteristic molecular weight M_c ($=10^4$). τ_{Dn} is proportional to $M^{3.7}$ in the region $M > M_c$ and $M^{2.0}$ in the region $M < M_c$. The $M^{3.7}$ dependence has been explained semiquantitatively by the tube theory.

(2) The distribution of the relaxation time for the normal mode process can be also explained by the tube theory considering three types of motions, i.e., the chain end motion, the Rouse mode due to stretching of the chain in

the tube, and the tube disengagement process.

(3) The dipole moment per unit contour length of *cis*-PI is 3.31×10^{-12} to 4.80×10^{-12} cgs esu depending on the assumption of the internal field. The perpendicular dipole component per the repeat unit was determined to be 0.21 D.

Acknowledgment. We thank Professor Masao Doi of Tokyo Metropolitan University for helpful discussion. We also thank Dr. Kazuyuki Tatsumi of Osaka University, who kindly made the computer calculation of the dipole moment of *cis*-Polyisoprene. This work was supported partly by the Institute of Polymer Research, Osaka University.

Registry No. Polyisoprene (homopolymer), 9003-31-0.

References and Notes

(1) Stockmayer, W. H. *Pure Appl. Chem.* **1967**, *15*, 539.
(2) North, A. M. *Chem. Soc. Rev.* **1972**, *1*, 49.
(3) Adachi, K.; Kotaka, T. *Macromolecules* **1983**, *16*, 1936.
(4) Rouse, P. E. *J. Chem. Phys.* **1953**, *21*, 1272.
(5) Zimm, B. H. *J. Chem. Phys.* **1956**, *24*, 269.
(6) Adachi, K.; Kotaka, T. *Macromolecules* **1984**, *17*, 120.
(7) Stockmayer, W. H.; Baur, M. E. *J. Am. Chem. Soc.* **1964**, *86*, 3485.
(8) Baur, M. E.; Stockmayer, W. H. *J. Chem. Phys.* **1965**, *43*, 4319.
(9) Stockmayer, W. H.; Burke, J. J. *Macromolecules* **1969**, *2*, 647.
(10) Jones, A. A.; Stockmayer, W. H.; Molinari, R. J. *J. Polym. Sci., Polym. Symp.* **1976**, *No. 54*, 227.
(11) North, A. M.; Phillips, P. J. *Trans. Faraday Soc.* **1968**, *64*, 3235.
(12) Hirose, M.; Yamakawa, N.; Araki, K.; Imamura, Y. *Rep. Prog. Polym. Phys. Jpn.* **1976**, *20*, 117.
(13) Ferry, J. D. "Viscoelastic Properties of Polymers"; Wiley: New York, 1961.
(14) Graessley, W. W. *Adv. Polym. Sci.* **1974**, *16*, 1.
(15) de Gennes, P.-G. *J. Chem. Phys.* **1971**, *55*, 572.
(16) de Gennes, P.-G. "Scaling Concepts in Polymer Physics"; Cornell University Press: Ithaca, NY, 1979.
(17) Doi, M.; Edwards, S. F. *J. Chem. Soc., Faraday Trans. 2* **1978**, *74*, 1789, 1802, 1818.
(18) McCrum, N. G.; Read, B. E.; Williams, G. "Anelastic and Dielectric Effects in Polymeric Solids"; Wiley: New York, 1967.
(19) Morton, M.; Fetters, L. J. *Rubber Chem. Technol.* **1975**, *48*, 359.
(20) Adachi, K.; Hirose, Y.; Ishida, Y. *J. Polym. Sci., Polym. Phys. Ed.* **1975**, *13*, 1491.
(21) Vogel, H. *Z. Phys.* **1921**, *22*, 645.
(22) Tamman, G.; Hesse, W. *Z. Anorg. Allg. Chem.* **1926**, *156*, 245.
(23) Nemoto, N.; Moriwaki, M.; Odani, H.; Kurata, M. *Macromolecules* **1971**, *4*, 215.
(24) Nemoto, N.; Odani, H.; Kurata, M. *Macromolecules* **1972**, *5*, 531.
(25) Havriliak, S.; Negami, S. *J. Polym. Sci., Part. C* **1966**, *No. 14*, 99.
(26) Flory, P. J.; Fox, T. G. *J. Am. Chem. Soc.* **1951**, *73*, 1907, 1909, 1915.
(27) Poddubnyi, I. Y.; Ehrenberg, E. G. *J. Polym. Sci.* **1962**, *57*, 545.
(28) Le Fevre, R. J. W. "Dipole Moment"; Wiley: New York, 1964.
(29) Adachi, K.; Okazaki, H.; Kotaka, T., unpublished data.
(30) Mark, J. E. *J. Am. Chem. Soc.* **1966**, *88*, 4354.
(31) Smyth, C. P. *J. Am. Chem. Soc.* **1929**, *51*, 2380.
(32) Tatsumi, K., unpublished data.
(33) Berry, G. C.; Fox T. G. *Adv. Polym. Sci.* **1969**, *6*, 1.
(34) Doi, M. *J. Polym. Sci., Polym. Phys. Ed.* **1983**, *21*, 667.
(35) Cole, R. H. *J. Chem. Phys.* **1975**, *42*, 637.
(36) Doi, M., private communication.
(37) van Krevelen, D. W. "Properties of Polymers", 2nd ed.; Elsevier: Amsterdam, 1976.

Oriented Crystallization of Cross-Linked Polybutadiene Rubber. 2. Small-Angle and Wide-Angle X-ray Scattering

Takeji Hashimoto,* Kenji Saijo, Michał Kość,† and Hiromichi Kawai

Department of Polymer Chemistry, Faculty of Engineering, Kyoto University, Sakyo-ku, Kyoto 606, Japan

Andrzej Wasiak and Anderzej Ziabicki

Polish Academy of Sciences, Institute of Fundamental Technological Research, 00-049 Warszawa, Poland. *Received November 14, 1983*

ABSTRACT: Effects of amorphous chain orientation on the orientation distribution of crystallites formed by oriented crystallization of cross-linked *cis*-1,4-polybutadiene were investigated by using small-angle (SAXS) and wide-angle X-ray scattering (WAXS). Orientation distribution of lamellar normals $q_l(\psi)$ and of the reciprocal lattice vectors, $q_{hkl}(\psi)$ of the (110) and (020) planes, were presented as functions of crystallization temperature (T_c = 240–260 K) and draw ratios (λ = 1.6–3.0). The results indicate that the higher the temperature T_c and the larger the draw ratio λ, the sharper are the orientation distributions $q_l(\psi)$ and $q_{hkl}(\psi)$ produced. It has been shown that the observed phenomena can be understood on the basis of either of the two asymptotic crystallization theories: (i) equilibrium theory of crystallization in a phantom network and (ii) kinetic theory of nucleation in a system of asymmetric elements.

I. Introduction

Oriented crystallization of cross-linked polymers has been of interest to theoreticians and experimentalists since the beginning of polymer science. It involves a fundamental problem concerning the effect of molecular orientation (i.e., a reduction of conformational entropy of long-chain molecules) on phase transition. The fundamental molecular theories of oriented crystallization include the theory of Flory,[1] developed later by Smith[2] and Wu,[3] theories of Krigbaum and Roe,[4] Gaylord,[5] Baranov and Elyashevich,[6] Jarecki and Ziabicki,[7,36] and Allegra.[8] Experimental aspects of the problem have been investigated by Gehman and Field,[9] Kawai,[10] Keller,[11] Luch and Yeh,[12] Cesari,[13] and others.[14-20]

The aim of this work was to study crystallite orientation in isothermally crystallized cross-linked *cis*-1,4-polybutadiene in the stretched state and to explain its nature on the basis of equilibrium and kinetic theories. Crystallite orientation in polymers crystallized under molecular ori-

† On leave from the Polish Academy of Sciences.

0024-9297/85/2218-0472$01.50/0